Development of the Timing System for the Bunch-to-Bucket Transfer between the FAIR Accelerators

J. Bai[1,2*] and T. Ferrand[1,3], O. Kester[1,4], D. Ondreka[1], D. Beck[1], C. Prados[1,?]
1. GSI Helmholtzzentrum für Schwerionenforschung, 64291 Darmstadt, Germany
2. IAP, Goethe University Frankfurt am Main, 60439 Frankfurt am Main, Germany
3. TEMF, Technique University Darmstadt, 64291 Darmstadt, Germany
4. TRIUMF, 4004 Wesbrook Mall Vancouver, BC V6T 2A3 Canada

The Facility for Antiproton and Ion Research (FAIR) project is aiming at providing high-energy beams of ions of all elements from hydrogen to uranium, as well as antiprotons and rare isotopes with high intensities. The existing accelerator facility of GSI Helmholtz center for Heavy Ion Research GmbH (short: GSI) and the future FAIR facility employ a variety of circular accelerators like heavy ion synchrotrons (the SIS18 and the SIS100) and storage rings (the experimental storage ring ESR, the CRYRING@ESR, the collector ring CR and the high energy storage ring HESR) for the preparation of secondary beams and experiments. Bunches are required to be transferred into rf buckets among GSI and FAIR circular accelerators for different purposes. All this imposes new requirements on the bunch-to-bucket transfer system. These requirements include the bunch-to-bucket transfer between two rings with an arbitrary ratio in their circumference, two synchronization methods (the phase shift method and the frequency beating method), the required bunch-to-bucket transfer time 10 ms, the tolerable bunch-to-bucket injection center mismatch less than $\pm 1^\circ$ and the primary beam transfer as well as the secondary beam. In order to fulfill these requirements, a completely new and unique FAIR bunch-to-bucket transfer system will be developed. The presentation of the concept of the system and the systematic investigation from timing perspective are the purpose of this paper. The concept and basic procedure of the system first of all are presented. Afterwards, a systematic investigation from the beam dynamics, timing requirement of the transfer and kicker trigger perspectives is analyzed. Finally, the application of the system for all FAIR use cases with the frequency beating method is summarized.

PACS numbers: 29.20.D-. 29.27.Ac. 07.05.Dz

I. INTRODUCTION

The bunch-to-bucket (B2B) transfer is a process that bunches circulating in the source circular accelerator (short: ring) are transferred into the center of rf buckets of the target ring. This transfer method has already been used in several accelerator institutes worldwide for specific purposes. CERN, the European Organization for Nuclear Research, makes use of the B2B transfer to produce high energy beams for scientific research. The Large Hadron Collider (LHC) is supplied with 7 TeV high energy proton beam from the injector chain Linac2 - Proton Synchrotron (PS) Booster - PS - Super Proton Synchrotron (SPS) and with 2.76 TeV/u high energy heavy ion beam from the injection chain Linac3 - Low Energy Ion Ring (LEIR) - PS - SPS [1]. The transfer among CERN rings is realized by the B2B transfer. The CERN B2B transfer system is based on the direct transmission of the revolution frequency signal from the target to the source ring around the campus for the bucket counting and synchronization. In order to synchronize two rings, beam is moved to off-momentum by adjusting frequency (magnetic field is constant). The phase difference between two rings varies periodically. Then the azimuth error between two rings is measured and beam is moved back to the reference momentum when beam is at correct azimuth. The complete synchronization process takes about 500 ms [2]. The Japan Proton Accelerator Complex (J-PARC) uses the B2B transfer to transfer proton beams from the Rapid Cycle Synchrotron (RCS) to the Main Ring (MR) to gain higher energy for the further production of the desired secondary particle beam [3]. In the injection period of the MR, the rf system provides rf signals of a fixed frequency. The information (the phase of the MR rf system, the empty bucket tag) sent from the MR to the RCS. The positions of bunches in the RCS are controlled during acceleration by using the phase information from the MR so that two bunches are in the proper phase at the top energy. The tag information gives the proper timing for triggering the kickers at the time of the empty buckets in the MR [4].

FAIR is a new international accelerator facility under construction at GSI. It is aiming at providing high-energy beams of ions of all elements from hydrogen to uranium with high intensities, as well as beams of rare isotopes and of antiprotons [5, 6]. The FAIR accelerators will be supplied with ion beams by the GSI accelerator facility, which comprises the injectors for the FAIR accelerators. The injection chain consists of the linear accelerator UNILAC and the heavy ion synchrotron SIS18. In addition, the GSI accelerator facility comprises the ESR and the CRYRING@ESR (short: CRYRING), which complement the planned accelerators of FAIR. The FAIR accelerator complex in its start version will consist of the

* Email: baijiaoni1314@gmail.com

SIS100, the CR and the HESR. For FAIR, the intermediate charge state ions are used to increase the beam intensity by reducing space charge at SIS18, causing the larger mass-to-charge ratio. However, the intermediate charge state ion beams can not be accelerated to high enough energy at the existing SIS18 due to the constraints of the magnetic rigidity. On the other hand, the intermediate charge state ion beams cause the dynamic vacuum challenge by their significantly enhanced cross section for ionization and their high potential for generating ion desorption driven vacuum instabilities. Hence, the SIS100 with a larger magnetic rigidity is required for the further acceleration. Beside, the perfect control over the dynamic vacuum at SIS100 realizes smaller cross sections for charge exchange and the special lattice design optimizes best control of the ionization beam loss [7, 8]. Furthermore, with the double ring facility, high average intensity heavy ion beams can be provided with the help of the beam stacking by the multiple injection. The CR will accumulate the secondary beams and improve their quality by stochastic cooling. The storage ring HESR will host a large fraction of the experiment platforms with a variety of different experiments [9, 10]. The high energy antiproton/rare isotope beam chain is composed of the UNILAC - SIS18 - SIS100 -antiproton target/superconducting fragment separator- CR - HESR and the lower energy chain cascades of UNILAC - SIS18 -fragment separator- ESR - CRYRING.

Although an implementation of the B2B transfer from the SIS18 to the ESR exists, this solution is not applicable for the new FAIR accelerator complex, because it is realized based on the GSI control system [11], which will be replaced by a new control system for FAIR. The FAIR control system is based on the sub-nanosecond synchronization White Rabbit (WR) network. Besides, the existing B2B transfer does not support the B2B transfer between two rings with an integer circumference ratio.

In the following the requirements for the FAIR B2B transfer system is listed. In Sec. III the concept of the FAIR B2B transfer system is introduced together with the basic procedure. The FAIR B2B transfer system focus first of all on the transfer from the SIS18 to the SIS100. Hence, the Sec. IV is concerned with the analysis of two synchronization methods from the beam dynamics for the B2B transfer from the SIS18 to the SIS100. In Sec. V, the timing constraints of the system is presented. The different trigger scenarios of the SIS18 extraction and SIS100 injection kickers are discussed in Sec. VI. Afterwards the application of the system for FAIR use cases with the frequency beating method is presented in Sec. VII.

II. REQUIREMENTS FOR THE FAIR B2B TRANSFER SYSTEM

The FAIR B2B transfer system shall fulfill the requirements for all FAIR use cases. It should achieve the FAIR B2B transfers with a tolerable bunch-to-bucket injection center mismatch (e.g. $\pm 1^\circ$ for most FAIR use cases) and within an upper bound time (e.g. 10 ms for most FAIR use cases). It must support both the phase shift and frequency beating methods (see Sec. III). It must be flexible to support the beam transfer between two rings with an arbitrary ratio in their circumference and several B2B transfers running at the same time, e.g. the B2B transfer from the SIS18 to the SIS100 and at the same time the B2B transfer from the ESR to the CRYRING. It should be capable to transfer beam of different ion species from one machine cycle to another. It supports the beam transfer via the the antiproton (pbar) target, the fragment separator (FRS) and the superconducting fragment separator (Super-FRS). It must support various complex bucket filling patterns, e.g. eight out of ten SIS100 buckets are filled by four SIS18 batches, each of two bunches. In addition, it should coordinate with the machine protection system, which protects the SIS100 and subsequent accelerators or experiments from beam induced damage.

III. CONCEPT OF THE FAIR B2B TRANSFER SYSTEM

The new FAIR B2B transfer system relies on the FAIR technical basis, the FAIR timing and control system and the low-level radio frequency (LLRF) system. The FAIR control system takes advantage of several collaborations with CERN by using, adapting and improving framework solutions like the settings management framework LSA, the front-end software framework FESA and the WR based timing system as core components [12]. The General Machine Timing (GMT) system synchronizes all Front End Controllers (FEC) with nanosecond accuracy over the whole FAIR campus and distributes timing messages to all FECs via the reliable and robust WR network and controls all FECs to execute real-time actions at a designated time [13]. The GMT system mainly consists of a data master (DM), the WR network and FECs. The DM defines the accelerator schedule. The Scalable Control Unit (SCU) [14] is a new generation of the standard FEC for the FAIR control system, which provides a compact and flexible solution for controlling all types of accelerator equipment. For the synchronization of the LLRF system, the GMT system is complemented and linked to the Bunch Phase Timing System (BuTiS) [15, 16], which serves as a campus-wide clocks distribution system with sub nanosecond resolution and stability over distances of several hundred meters. The LLRF system synchronizes cavities in every ring by the reference rf signal distribution system (short: rf system) [17].

In order to complete the B2B transfer, first of all, the rf systems of the source and target rings must be correctly phase aligned. Secondly, the trigger for the extraction and injection kicker magnets must be synchronized with the beam. Finally the time point of the actual beam in-

jection into the target ring must be indicated to enable beam instrumentation devices to measure the properties and the behavior of the beam directly after the injection [18]. In the following, the realization of these three functionalities will be presented. For the B2B transfer, there is a so-called B2B transfer master, which is responsible for the data collection of two rings, the data calculation, the data redistribution and the B2B transfer status check. For the sake of simplicity, the source ring works as the B2B transfer master.

A. Phase Alignment

In order to realize the phase alignment, the phase difference $\Delta\phi$ between the two rf systems of two rings must be obtained. The phase difference is indirectly measured via a FAIR campus wide distributed reference signal synchronized with BuTiS clocks.

$$\begin{aligned}\Delta\phi &= (\Delta\phi_1 - \Delta\phi_2) \mod 2\pi \\ &= [2\pi(f_1 - f_{ref})t + \phi_1] \\ &- [2\pi(f_2 - f_{ref})t + \phi_2] \mod 2\pi \\ &= [2\pi(f_1 - f_2)t + \phi_1 - \phi_2] \mod 2\pi\end{aligned} \tag{1}$$

where ϕ_1 and ϕ_2 are the initial phases of the two rf systems of the source and target rings, f_1 and f_2 the frequencies of the two rf systems, f_{ref} the frequency of the reference signal and $\Delta\phi_1$ and $\Delta\phi_2$ the phase difference between the two rf systems and the reference signal.

For the phase difference, there are two scenarios according to the relation between f_1 and f_2. When f_1 equals to f_2, $\Delta\phi$ is constant. In order to change the phase difference for the phase alignment, the phase of either (or both) rf system must be shifted by modulating the frequency of the rf system away from the reference value for a specific period of time and then modulating back. This is called "phase shift".

When f_1 and f_2 are slightly different, $\Delta\phi$ is a periodic function whose rate is the difference between two frequencies. This is called "frequency beating". The periodically variable rate is called the "beating frequency", $\Delta f = |f_1 - f_2|$. The beating period is defined as a period of time for the periodical variation, namely $1/\Delta f$. Within one beating period, there exists a time point, which corresponds to a correct phase difference between the two rf systems, namely the phase alignment.

The phase alignment is realized based on two identical or two slightly different frequencies. These two frequencies are called "synchronization frequencies", denoted as f^X_{syn}, where X indicates the ring. The phase difference between two synchronization frequency is denoted as $\Delta\phi_{syn}$. The number of circulating buckets is determined by the harmonic number and the cavity rf frequency is the harmonic number times of the revolution frequency. The cavity rf frequency is denoted as f^X_{rf} and the revolution frequency f^X_{rev}. The FAIR LLRF system produces the revolution frequency as the 1^{st} harmonic and supports not only the integer multiple but also the fractional multiple of the revolution frequency. For all FAIR use cases, two synchronization frequencies are an integer multiple of the same or slightly different derived rf frequencies, which are the fraction of the revolution frequencies.

$$f^X_{syn} = Y \cdot f^X_{rev}/m \tag{2}$$

where f^X_{rev}/m represents the fraction of the revolution frequency and both m and Y are positive integers, which are determined by the circumference ratio and the harmonic numbers.

For FAIR use cases with an integer ratio in their circumference, there is an integer multiple relationship between two revolution frequencies. In this case, two identical synchronization frequencies are integer times of the revolution frequencies, namely $m = 1$ in eq. 2. For example, the H^+ B2B transfer from the SIS18 to the SIS100 has $f^{SIS100}_{syn} = 5f^{SIS100}_{rev}$ and $f^{SIS18}_{syn} = f^{SIS18}_{rev}$, see Fig. 1. For detailed parameters of the FAIR B2B transfer from the SIS18 to the SIS100, please see Appendix. B 1.

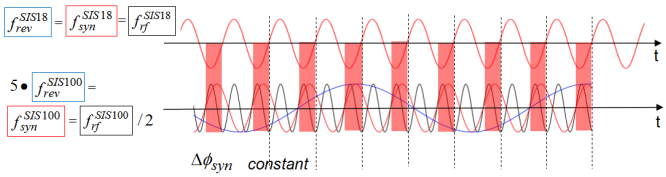

FIG. 1. Example of the synchronization frequencies in the scenario of an integer circumference ratio between two rings. *The example is the FAIR use case of the H^+ B2B transfer from SIS18 to SIS100.*

For FAIR use cases with a close to an integer ratio in their circumference, there is a close to an integer multiple relationship between two revolution frequencies. In this case, two slight different synchronization frequencies are integer times of the revolution frequencies, namely $m = 1$ in eq. 2. For example, four bunches transfer from the SIS18 to the ESR has $f^{SIS18}_{syn} = 4f^{SIS18}_{rev}$ and $f^{ESR}_{syn} = 2f^{ESR}_{rev}$, see Fig. 2. For detailed parameters of the FAIR B2B transfer from the SIS18 to the ESR, please see Appendix. B 2.

For quite many FAIR use cases with the ring circumference ratio far away from an integer, there are big different revolution frequencies, two synchronization frequencies are calculated as $Y \cdot f^X_{rev}/m$. For example, the B2B transfer from the CR to the HESR has $f^{CR}_{syn} = 2 \cdot f^{SIS100}_{rev}/26$ and $f^{HESR}_{syn} = 2 \cdot f^{CR}_{rev}/10$, see Fig. 3. For detailed parameters of the FAIR B2B transfer from the CR to the HESR, please see Appendix. B 5.

For the 1^{st} scenario, two synchronization methods are available for the phase alignment of the two rf systems, the phase shift method and the frequency beating method. For the 2^{nd} and 3^{rd} scenarios, only the frequency beating method is available. Both methods provide a time frame for the B2B transfer, within

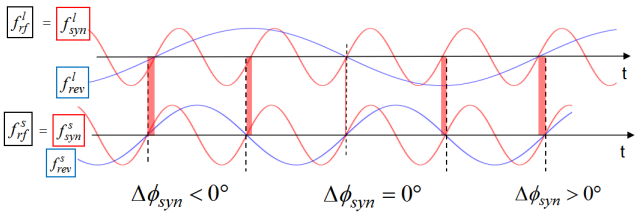

FIG. 2. Example of the synchronization frequencies in the scenario of a close to an integer circumference ratio between two rings.

The example is the FAIR use case of four bunches transfer from SIS18 to ESR.

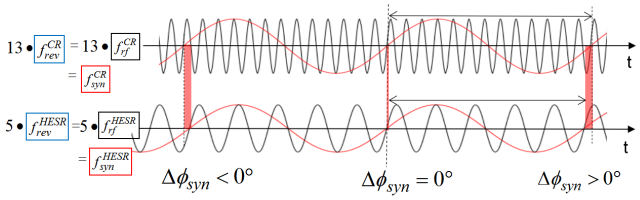

FIG. 3. Example of the synchronization frequencies in the scenario of a far away from an integer circumference ratio between two rings.

The example is the FAIR use case of the B2B transfer from CR to HESR.

which bunches are transferred into buckets with a certain bunch-to-bucket injection center mismatch smaller than a given upper bound (e.g. $\pm 1°$). This time frame is called the synchronization window.

1. *Phase shift method*

The required phase shift $\Delta\phi_{syn}$ depends on the frequency modulation Δf_{rf} and the duration T.

$$\Delta\phi_{syn} = 2\pi \int_{t_0}^{t_0+T} \Delta f_{rf}(t)dt \tag{3}$$

where t_0 is the start time of the phase shift.

During the phase shift process, beam is moved to off-momentum by adjusting frequency (magnetic field is constant) and moved back to the reference momentum after the certain duration. After the phase shift, bunches of the source ring are phase aligned with buckets of the target ring. The synchronization window is defined as the time frame after the rf frequency modulation, see Fig. 4.

The phase shift process must be performed slowly enough to preserve the longitudinal emittance. In summary the rf frequency modulation function must meet the following requirements.

- There is a maximum value for Δf_{rf} , which is constrained by the maximum tolerable relative momentum shift $\Delta p/p$ [19]. $\Delta p/p$ is constrained by the semi-aperture required for the beam and the dispersion function.

$$\frac{\Delta p}{p} = \frac{1}{\frac{1}{\gamma^2} - \alpha_p} \cdot \frac{\Delta f_{rf}}{f_{rf}} \tag{4}$$

where γ is the relativistic factor, which measures the total particle energy in units of the particle rest energy and α_p is the momentum compaction factor.

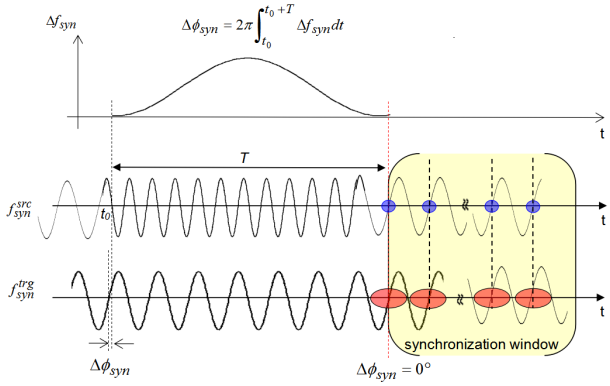

FIG. 4. Example for the phase shift method with a sinusoidal rf frequency modulation.

Blue dots represent bunches of the source ring and red dots buckets of the target ring.

- The 1^{st} time derivative of Δf_{rf} must be continuous, so that the synchronous phase changes continuously for the beam to follow.

$$\begin{aligned} V_0\phi_s \approx V_0 \sin\phi_s &= 2\pi R\rho\dot{B} = \frac{2\pi RB\rho}{p}\frac{d\Delta p}{dt} \\ &= \frac{2\pi RB\rho}{(1/\gamma^2 - \alpha_p)f_{rf}}\frac{d\Delta f_{rf}}{dt} \end{aligned} \tag{5}$$

where V_0 is the amplitude of the rf voltage, ϕ_s the synchronous phase, B the magnetic field, ρ the bending radius of a particle immersed in a magnetic field B, R the average orbit radius and q the charge of a particle.

- The 1^{st} time derivative of Δf_{rf} must be small enough to guarantee buckets size big enough to capture bunches. The ratio of the bucket size of a running bucket to that of a stationary bucket is called the "bucket area factor", denoted as α_b [20].

$$\alpha_b(\phi_s) \approx \frac{1-\phi_s}{1+\phi_s} \tag{6}$$

- The 2^{nd} time derivative of Δf_{rf} must be small enough, so that the change rate of the synchronous phase is slow enough for the beam to follow. The 2^{nd} time derivative of Δf_{rf} is reflected by the parameter of the adiabaticity ε [21].

$$\varepsilon \approx \frac{1}{2\omega_s}|\phi_s\dot{\phi}_s| \tag{7}$$

where ω_s is the angular synchrotron frequency.

In order to accomplish the phase alignment as fast as possible, the phase shift will be conducted backward and forward for FAIR. Therefore a phase shift of up to $\pm\pi$ will be considered for rf systems with regard to the synchronization frequency f^X_{syn}. Besides, a normalized frequency modulation profile $f_{normalized}$ for π must be precalculated, which meets the requirements mentioned above. The actual frequency modulation profile f_{actual} is decided by $f_{normalized}$ and the required phase shift $\Delta\phi_{syn}$.

$$f_{actual}(t) = \frac{\Delta\phi_{syn}}{\pi} f_{normalized}(t) \tag{8}$$

2. *Frequency beating method*

The frequency beating method uses two slightly different synchronization frequencies. When two synchronization frequencies are slightly different, two rf systems are beating automatically. When they are identical, one (or both) rf system is detuned to achieve the beating. The frequency is detuned at constant energy by changing the radius and the magnetic field ($\Delta p/p = 0$). The frequency detuning is constrained by the relative radius excursion $\Delta R/R$ [19].

$$\frac{\Delta R}{R} = -\frac{\Delta f_{rf}}{f_{rf}} \tag{9}$$

The synchronization window is defined as a symmetric time frame with respect to the time, when the phase difference between two synchronization frequencies is closest to the required phase difference, see Fig. 5. The length of the synchronization window is defined in the later part.

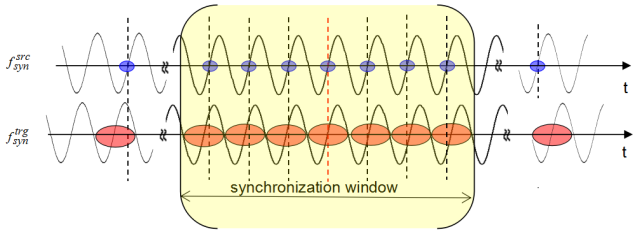

FIG. 5. Illustration of the frequency beating method. Blue dots represent bunches of the source ring and red dots buckets of the target ring.

In conclusion, the frequency beating method is preferable for the FAIR project, because it is applicable for the B2B transfer with either an integer or non integer circumference ratio. In addition, it reduces the duration of the B2B transfer process (e.g. 10 ms is an upper bound for most FAIR use cases), because the rf frequency detuning is executed during the rf acceleration ramp. For the phase shift method, the rf frequency modulation must be executed slowly enough at the rf flattop for beams to follow according to the criteria. The phase shift method therefore needs much longer time to be executed. However, there are also some advantages of the phase shift method. The synchronization window is relatively long and the B2B injection center mismatch is approximately 0°. Besides, the duration of the rf frequency modulation is known in advance and the time point for the transfer is predictable. The phase of the rf system can jump to a desired value, when there is no bunch at the ring.

B. Trigger of Extraction and Injection Kickers

The phase alignment provides a synchronization window, within which bunches can be transferred into buckets with the B2B injection center mismatch smaller than an upper bound (e.g. ±1°). This process is called "coarse synchronization". Furthermore, within the synchronization window the extraction kicker must kick bunches exactly the time-of-flight earlier before a specific bucket passes the injection kicker. This process is called "fine synchronization". The fine synchronization requires the kicker firing based on a bucket indication signal for the 1^{st} bucket of the target ring plus a fixed delay (e.g. the time-of-flight) [18]. The combination of two synchronization process achieves that bunches are injected into correct buckets. Fig. 6 illustrates two synchronization processes.

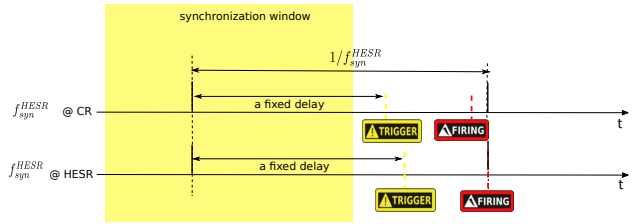

FIG. 6. Two synchronization processes. The example is the FAIR use case of the B2B transfer from CR to HESR. The frequency of the bucket indication signal equals to the HESR synchronization frequency.

For FAIR use cases, either m/Y or Y/m is an integer for $f^X_{syn} = Y \cdot f^X_{rev}/m$. In other words, either the revolution period is an integer multiple of the period of the synchronization frequency or the period of the synchronization frequency is an integer multiple of the revolution period. The bucket indication signal needs to indicate not only the 1^{st} bucket of the target ring, but also the phase alignment with the rf system of the source ring, therefore the bucket indication signal, f_{bucket}, has the smaller value of f^{trg}_{rev} or f^{trg}_{syn}. For example, the H^+ B2B transfer from the SIS18 to the SIS100 has $f_{bucket} = f^{trg}_{rev}$ (see Fig. 7) and the B2B transfer from the CR to the HESR has $f_{bucket} = f^{trg}_{syn}$ (see Fig. 8). The length of the synchronization window is one period of the bucket indication signal.

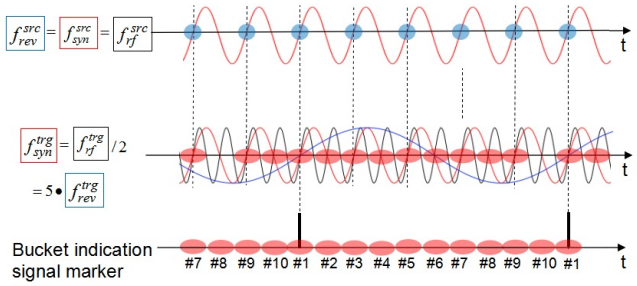

FIG. 7. Frequency of the bucket indication signal equals to the revolution frequency of the target ring.

This example is the FAIR use case of the H^+ B2B transfer from SIS18 to SIS100. The correct phase alignment of the two rf systems is assumed with $\Delta\phi_{syn} = 0°$ and only the buckets with the odd number (e.g. ♯1, ♯3) are to be filled in this example.

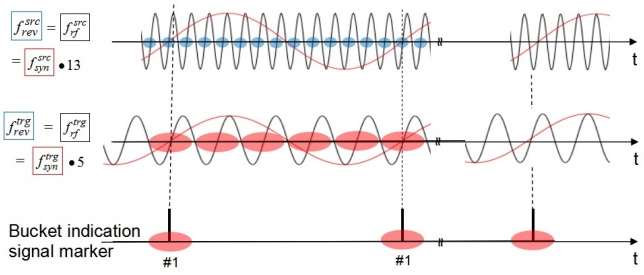

FIG. 8. Frequency of the bucket indication signal equals to the synchronization frequency of the target ring.

This example is the FAIR use case of the B2B transfer from CR to HESR.

C. Beam Indication for Beam Instrumentation Devices

Specific SCUs for the B2B transfer are required, including a B2B source SCU and a source trigger SCU at the source ring and a B2B target SCU and a target trigger SCU at the target ring. The B2B source SCU works as the B2B transfer master. The B2B target SCU is responsible for the phase measurement at the target ring. The source and target trigger SCUs are used to produce kicker trigger signals [18]. The calculation of the start of the synchronization window and the distribution of it in the format of the timing message to the WR network is one of the tasks of the multi-purpose B2B source SCU. The timing message will be received by SCUs of the beam instrumentation and the corresponding devices will be activated by the timing message at the start time point of the synchronization window. In addition, the message will also be received by the trigger SCUs, indicating the synchronization window. Within the window, the first bucket indication signal will be selected plus a fixed delay to produce the trigger signals.

D. Basic Procedure

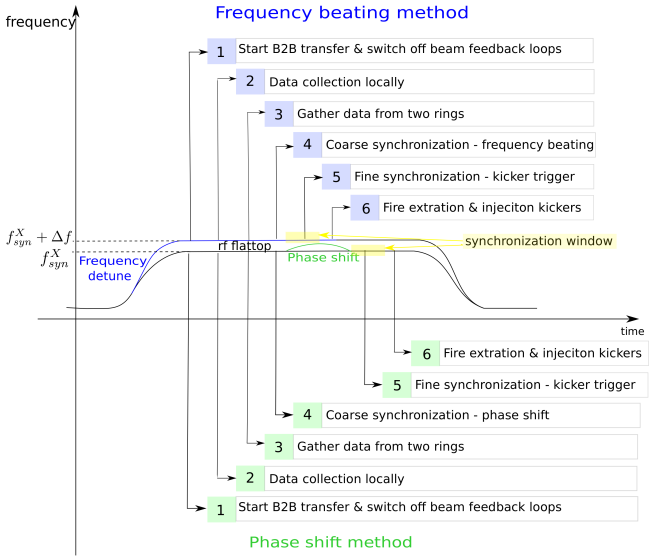

FIG. 9. Procedure of the B2B transfer within one acceleration cycle.

As illustrated here the procedure with the frequency beating method (blue, top) and that with the phase shift method (green, bottom).

Fig. 9 illustrates the basic procedure of the B2B transfer with two different synchronization methods. The yellow region shows the synchronization window. The B2B transfer process basically needs to follow the six steps [18].

IV. BEAM DYNAMICS ANALYSIS OF TWO SYNCHRONIZATION METHODS

The FAIR B2B transfer system focuses first of all on the transfer from SIS18 to SIS100, so the beam dynamics of SIS18 beams are analyzed. Because the most stringent requirement are from the lightest and heaviest ion species, the beam dynamics of the H^+ and U^{28+} beams are taken into consideration.

For the rf frequency modulation of the phase shift method ($\Delta B/B = 0$), the dispersion function is reflected in the relative momentum shift. The maximum tolerable relative momentum shift is decided by the semi-aperture $X_D(s)$ required for the beam and the dispersion function $D(s)$.

$$X_D(s) = D(s) \cdot \frac{\Delta p}{p}|_{\frac{\Delta B}{B}=0} \tag{10}$$

The maximum tolerable relative momentum of the H^+ beam and that of the U^{28+} beam of the SIS18 are same by coincidence, $\Delta p/p_{\_max} = \pm 0.008$.

For the frequency detuning of the frequency beating method ($\Delta p/p = 0$), the dispersion function is reflected

in the relative bending magnetic field shift.

$$X_D(s) = -D(s) \cdot \frac{\Delta B}{B}|_{\frac{\Delta p}{p}=0} \tag{11}$$

The maximum tolerable relative bending magnetic field shift of the H^+ beam and that of the U^{28+} beam of the SIS18 are minus of their maximum tolerant relative momentum shift, namely $\Delta B/B_{\_max} = -\Delta p/p_{\_max} = \pm 0.008$. The constraint on the displacement of the orbit length $\Delta L/L_{\_max}$ is obtained by

$$\frac{\Delta L}{L} = \begin{cases} \alpha_p \cdot \frac{\Delta p}{p} & \textit{Phase shift method} \\ -\alpha_p \cdot \frac{\Delta B}{B} & \textit{Frequency beating method} \end{cases} \tag{12}$$

where α_p is the momentum compaction factor. α_p equals to 0.01 for the SIS18 H^+ beam and 0.03 for the SIS18 U^{28+} beam [22].

The reasonable bucket size of a running bucket is larger than 80% of the size of a stationary bucket, namely the bucket area factor $\alpha_b(\phi_s) \geq 80\%$. Due to the constraint of the bucket size, the synchronous phase must stay within the range between $-6.4°$ and $+6.4°$ according to eq. 6.

The acceptable range of the parameters accompanying with the rf frequency modulation of the phase shift method for the SIS18 H^+ and U^{28+} beams are summarized in Tab. I and that accompanying with the frequency detuning of the frequency beating method are summarized in Tab. II. For detailed parameters of the SIS18 beams, please see Appendix B 1.

TABLE I. Acceptable range of the parameters accompanying with the rf frequency modulation of the phase shift method for the SIS18 H^+ and U^{28+} beams

$\Delta p/p_{\_max}$	$\Delta L/L_{\_max}$	$\alpha_b(\phi_s)_{\_min}$	ϕ_{s_max}
± 0.008	H^+ $\pm 0.80 \cdot 10^{-4}$ U^{28+} $\pm 2.40 \cdot 10^{-4}$	80%	$\pm 6.4°$

TABLE II. Acceptable range of the parameters accompanying with the frequency detune of the frequency beating method for the SIS18 H^+ and U^{28+} beams

$\Delta B/B_{\_max}$	$\Delta L/L_{\_max}$	$\alpha_b(\phi_s)_{\_min}$	ϕ_{s_max}
± 0.008	H^+ $\pm 0.80 \cdot 10^{-4}$ U^{28+} $\pm 2.40 \cdot 10^{-4}$	80%	$\pm 6.4°$

A. Beam Dynamics of Phase Shift Method

In order to guarantee a bucket area factor larger than 80% and an adiabaticity smaller than 10^{-4}, for the SIS18 200 MeV/u U^{28+} beam, $|\Delta f_{rf}|$ must be smaller than 8.137 kHz and $|\frac{d\Delta f_{rf}}{dt}|$ must be continuous and smaller than 95 Hz/ms and $|\frac{d^2\Delta f_{rf}}{dt^2}|$ must be smaller than 70 Hz/ms^2 according to eq. 4, 5 and 7. Complied with the above mentioned criteria, the following three examples of rf frequency modulation profiles with a certain duration T are analyzed first of all for the SIS18 U^{28+} beam. All three cases give the same phase shift of π. The phase shift is assumed to be achieved within 7 ms, namely $T = 7$ ms.

Case (1) is a sinusoidal modulation.

$$\Delta f_1(t) = \frac{1}{2T}[1 - cos(\frac{2\pi}{T}(t - t_0))] \qquad (t_0 + 0, t_0 + T] \tag{13}$$

Case (2) is a parabolic modulation, which consists of three parabolas and two lines between every two parabolas.

$$\Delta f_2(t) = \begin{cases} \frac{9}{T^3}(t - t_0)^2 & (t_0 + 0, t_0 + \frac{T}{6}] \\ \frac{1}{4T} + \frac{3}{T^2}(t - t_0 - \frac{T}{6}) & (t_0 + \frac{T}{6}, t_0 + \frac{2T}{6}] \\ \frac{1}{T} - \frac{9}{T^3}(t - t_0 - \frac{T}{2})^2 & (t_0 + \frac{2T}{6}, t_0 + \frac{4T}{6}] \\ \frac{3}{4T} - \frac{3}{T^2}(t - t_0 - \frac{4T}{6}) & (t_0 + \frac{4T}{6}, t_0 + \frac{5T}{6}] \\ \frac{9}{T^3}(t - t_0 - T)^2 & (t_0 + \frac{5T}{6}, t_0 + T] \end{cases} \tag{14}$$

Case (3) is also a parabolic modulation, consisting of three parabolas.

$$\Delta f_3(t) = \begin{cases} \frac{8}{T^3}(t - t_0)^2 & (t_0 + 0, t_0 + \frac{T}{4}] \\ \frac{1}{T} - \frac{8}{T^3}[(t - t_0) - \frac{T}{2}]^2 & (t_0 + \frac{T}{4}, t_0 + \frac{3T}{4}] \\ \frac{8}{T^3}[T - (t - t_0)]^2 & (t_0 + \frac{4T}{4}, t_0 + T] \end{cases} \tag{15}$$

Fig. 10 shows three rf frequency modulation profiles and

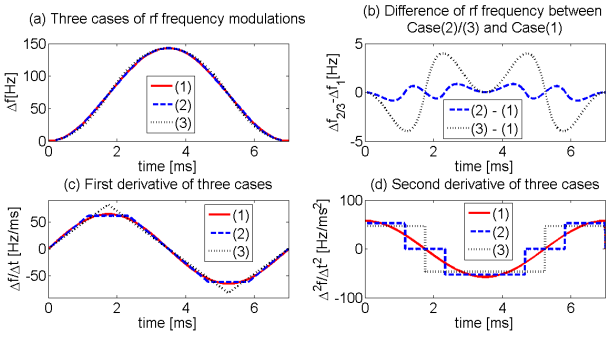

FIG. 10. Three rf frequency modulation cases.
(a) three rf frequency modulation cases (b) difference between case (2)/(3) and case (1) (c) the 1^{st} time derivative of three cases (d) the 2^{nd} time derivative of three cases

their 1^{st} and 2^{nd} time derivatives. The corresponding beam dynamics parameters are illustrated in Fig. 11 and summarized in Tab. III.

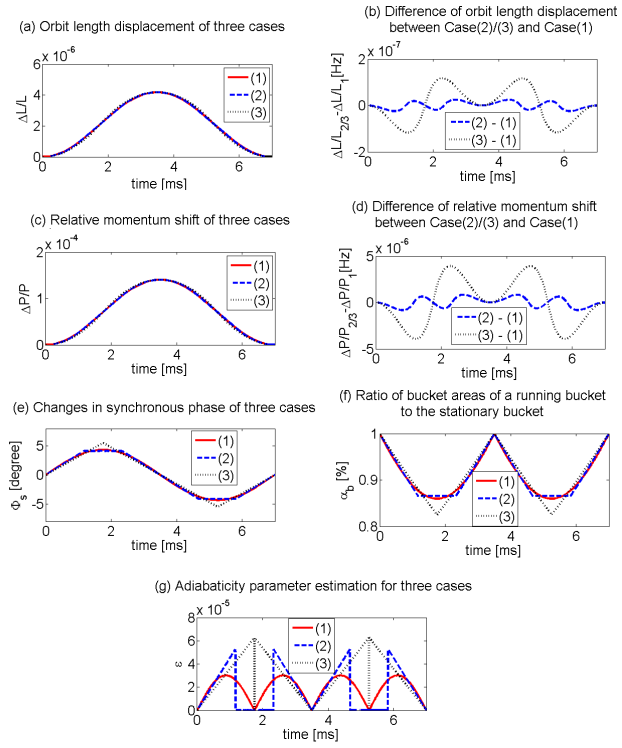

FIG. 11. Beam dynamics parameters of three cases. (a) orbit length displacement (b) difference of orbit length displacement between case (2)/(3) and case (1) (c) relative momentum shift (d) difference of relative momentum shift between case (2)/(3) and case (1) (e) changes in synchronous phase (f) ratio of bucket areas of a running bucket to the stationary bucket (g) adiabaticity

TABLE III. Corresponding beam dynamics parameters of three cases

	Case (1)	Case (2)	Case (3)
Maximum orbit length displacement	$4.18 \cdot 10^{-6}$	$4.18 \cdot 10^{-6}$	$4.18 \cdot 10^{-6}$
Maximum relative momentum shift	$1.40 \cdot 10^{-4}$	$1.40 \cdot 10^{-4}$	$1.40 \cdot 10^{-4}$
Synchronous phase	$< \pm 6.4°$	$< \pm 6.4°$	$< \pm 6.4°$
Minimum bucket area factor	86.0%	86.5%	82.5%
Maximum adiabaticity	$3.0 \cdot 10^{-5}$	$5.90 \cdot 10^{-5}$	$6.30 \cdot 10^{-5}$

According to the results, all three modulation profiles meet the requirements in Tab. I and keep the beam stable. However, compared with the parabolic modulation, the sinusoidal modulation has the smaller adiabaticity. Hence, the sinusoidal modulation is preferable for the phase shift method. The sinusoidal rf frequency modulation for the SIS18 200 MeV/u U^{28+} needs 7 ms for the phase shift of π.

For SIS18, the chromaticities $Q_x^{'}$ and $Q_y^{'}$ for the U^{28+} operation are -6.5 and -4.1. Using the chromaticity and the maximum momentum shift (see. Tab. III), the chromatic tune shifts ΔQ_x and ΔQ_y during rf modulations for three cases are calculated as

$$\Delta Q_x = Q_x' \frac{\Delta p}{p} = -6.5 \cdot 1.40 \cdot 10^{-4} = -9.10 \cdot 10^{-4} \quad (16)$$

$$\Delta Q_y = Q_y' \frac{\Delta p}{p} = -4.1 \cdot 1.40 \cdot 10^{-4} = -5.74 \cdot 10^{-4} \quad (17)$$

The chromatic tune shifts for three cases are negligible.

For the SIS18 4 GeV/u H^+ beam, $|\Delta f_{rf}|$ must be smaller than 283 Hz and $|\frac{d\Delta f_{rf}}{dt}|$ must be continuous and smaller than 1.9 Hz/ms and $|\frac{d^2\Delta f_{rf}}{dt^2}|$ must be smaller than 0.2 Hz/ms^2. With regard to these criteria, the sinusoidal modulation with $T = 50$ ms is used for the phase shift of π. The corresponding beam dynamics parameters are in Tab. IV.

TABLE IV. Parameters accompanying with a 50 ms sinusoidal modulation for the SIS18 H^+ beam

Relative momentum shift	Maximum orbit length displacement	Bucket size	Synchronous phase	Adiabaticity
$< 5.70 \cdot 10^{-4}$	$< 5.70 \cdot 10^{-6}$	$> 86\%$	$\pm 4.2°$	$< 0.80 \cdot 10^{-4}$

For the frequency modulation of the SIS18 H^+ beam, a longer period sinusoidal modulation (e.g. 50 ms) must be used for the beam performance consideration. For the SIS18 H^+ beam, the chromaticity $Q_x^{'}$ and $Q_y^{'}$ of H^+ is -7.5 and -4.4. Using the chromaticity and the maximum momentum shift (see. Tab. IV), the maximum chromatic tune shift ΔQ_x and ΔQ_y for the 50 ms sinusoidal modulation are calculated as

$$\Delta Q_x = Q_x' \frac{\Delta p}{p} = -7.5 \cdot 5.7 \cdot 10^{-4} = -4.28 \cdot 10^{-3} \quad (18)$$

$$\Delta Q_y = Q_y' \frac{\Delta p}{p} = -4.4 \cdot 5.7 \cdot 10^{-4} = -2.51 \cdot 10^{-3} \quad (19)$$

For the SIS18 4 GeV/u H^+ beam, the chromatic tune shifts for the 50 ms sinusoidal modulation are negligible.

B. Beam Dynamics of Frequency Beating Method

The frequency detuning has no influence on the chromaticity tune shift, because the momentum of the synchronous particle is not affected by the frequency detuning in order to guarantee the match of the extraction and injection energy.

For the frequency beating method, the rf frequency detuning is done at the end of the SIS18 rf acceleration

ramp. The SIS18 U^{28+} and H^+ acceptable displacement of the orbit length is $\pm 2.4 \cdot 10^{-4}$ and $\pm 0.80 \cdot 10^{-4}$, see Tab. II. Hence, the tolerable rf frequency change for 200 MeV/u U^{28+} and 4 GeV/u H^+ is calculated as

$$\frac{\Delta f_{rf}}{f_{rf}} = -\frac{\Delta L}{L} = \begin{cases} \mp 2.4 \cdot 10^{-4} & U^{28+} \\ \mp 0.80 \cdot 10^{-4} & H^+ \end{cases} \tag{20}$$

where the maximum rf frequency detuning approximates to 377 Hz and 109 Hz for the 200 MeV/u U^{28+} and 4 GeV/u H^+ beams.

V. TIMING CONSTRAINTS

The FAIR B2B transfer system has strict timing constraints. Because beam feedback loops (e.g. the beam phase control loop, the bunch-by-bunch longitudinal feedback loop) must be switched off before the B2B transfer, which modify the rf system according to the actual beam, the beam may be stable only for a short period of time. For most FAIR use cases, the upper bound time of the B2B transfer process is 10 ms.

The complete phase measurement needs approximately 500 µs. The longer time is used for the phase measurement, the more precise the measurement result will be [23]. The upper bound B2B related message transfer latency on the WR network is defined as 500 µs. So the transfer latency of the phase measurement from the B2B target SCU to the B2B source SCU is 500 µs in the worst case. The B2B source SCU needs about 100 µs for the data calculation, message creation and sending. The timing message containing the start of the synchronization window needs a 500 µs transfer latency on the network to the DM and another 500 µs further to SCUs responsible for beam instrumentation devices. Bunches must be transferred after beam instrumentation devices are activated. Hence, the start of the synchronization window must be $2 \cdot 500\,\mu s + 100\,\mu s + 2 \cdot 500\,\mu s = 2.1$ ms later than the start of the B2B transfer process.

In the following part, the WR network is characterized for the B2B transfer to meet the 500 µs timing constraint and the running time of the B2B related firmware running on the soft CPU, Latticemico32, of the SCU is checked for the timing constraints of 100 µs.

A. Characterization of the WR Network for the B2B Transfer

In order to meet the timing constraint of the B2B transfer, the data transfer on the WR network has an upper bound transfer latency of 500 us, 400 us of which can be used for the network transfer. Hence, the maximum number of WR switch layers between the B2B related SCUs must be defined. However, the more switches are used, the more optical fiber connections will be and the corresponding higher possibility of frame lost on the connections will happen. The maximum number of WR switch layers is constrained by the transfer latency and the tolerable lost frames. The optical fiber causes the bit error of the frame, which will be discarded by the switch. The lost frame caused by bit errors is measured by the frame error rate (FER), which is defined as the ratio between the number of lost frames caused by bit errors and the number of sent frames.

$$FER = n \cdot 10^{-12} \cdot 880 \tag{21}$$

where n is the number of WR switches used to establish the communication and the optical fiber's bit error rate is specified by the manufactures is 10^{-12} [24] and 880 is the length of an Ethernet frame including one timing message in the unit of bit [25].

For the B2B transfer, there are two types of messages. The 1^{st} type message is used to exchange data between two rings, which is sent by one SCU and sent to all other B2B related SCUs, e.g. the message of the phase measurement. The bandwidth is 25 kbit/s. The 2^{nd} type message is used to transfer data to the DM, which is sent by one SCU and sent only to the DM, e.g. the message of the start of the synchronization window. The bandwidth is 5 kbit/s. Both two types have the same format as the timing message with the length of 110 bytes. The tolerable FER is defined as one lost frame during a certain duration and calculated as

$$tolerable\_FER = \frac{1}{bandwith \cdot duration/880} \tag{22}$$

The requirements for these two types messages are listed here.

TABLE V. Requirements for two B2B types messages

	Maximum latency	Tolerable FER	Remark
1^{st} type	400 us	$6.70 \cdot 10^{-9}$	One lost frame every two months
2^{nd} type	400 us	$1.34 \cdot 10^{-9}$	

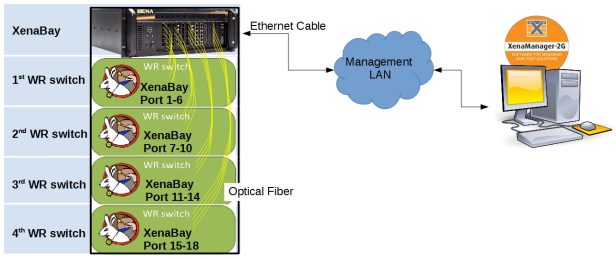

FIG. 12. An overview of the Xena's Layer 2-3 test platform for the WR network.

In the test, the Xena's Layer 2-3 test platform was used to characterize the properties of the WR network

for the B2B transfer. The Xena's Layer 2-3 test platform was used to configure and generate Ethernet traffic at the data link layer and network layer and then to analyze how WR network in response. Fig. 12 shows an overview of the Xena's Layer 2-3 test platform for the WR network. The test platform used the 4U XenaBay chassis which was equipped with an extensive range of copper and optical Gigabit Ethernet test modules. In the test, the test modules used 18 AXGE-1254 transceivers, 1.25 Gbps single fiber bidirectional small form-factor pluggable (SFP), to connect to ports of four WR switches via a G.652.B type single mode fibers. The chassis and test modules were controlled via Xena Manager-2G, a free Windows GUI client, which can be used to manage test equipment and execute test remotely. The test is used to identify the tolerable number of WR switch layers for the B2B transfer.

According to the importance of the network traffic, the prioritization of WR network traffic is implemented based on the virtual LAN (VLAN) technology. Control messages must be delivered deterministically and with very low loss, which schedules the real-time acceleration cycle. Hence, they are assigned to a VLAN with the highest priority, as well as the 2^{nd} type B2B message. Besides, messages used for the B2B related data exchange are assigned to a specific B2B VLAN with the secondary priority in order to reduce the network traffic. In addition, management messages are assigned to another VLAN with the lowest priority [26]. For more details of the traffic produced by XenaBay ports, please see Appendix A.

The 1^{st} type B2B messages are produced by one XenaBay's port and transferred via all four WR switches. After each switch, messages are received by another XenaBay's port. The transfer latency of the message via different number of switch layers is measured. Tab. VI shows the 45 days test result.

TABLE VI. Maximum frame transfer latency of the 1^{st} type B2B messages

Number of switch layers	one	two	three	four
Maximum transfer latency	28 µs	34 µs	37 µs	41 µs

The 2^{nd} type B2B messages are produced by one XenaBay's port and transferred via all four WR switches to another XenaBay's port. The transfer latency of the message via four switch layers, 23 µs, is measured in the 45 days test.

Based on the transfer latency requirement, the tolerable number of switch layers for the 1^{st} and 2^{nd} type B2B messages are calculated as

$$\frac{400\,\mu s}{28\,\mu s/\text{switch}} > 13 \tag{23}$$

$$\frac{400\,\mu s}{23\,\mu s/4\_\text{switch}} \cdot 4 > 67 \tag{24}$$

According to the tolerable FER requirement, the maximum number of switch layers for two types are calculated by eq. 21.

$$n_{1^{st}} = \frac{FER}{880 \cdot 10^{-12}} = \frac{6.70 \cdot 10^{-9}}{880 \cdot 10^{-12}} \approx 8 \tag{25}$$

$$n_{2^{nd}} = \frac{FER}{880 \cdot 10^{-12}} = \frac{1.34 \cdot 10^{-9}}{880 \cdot 10^{-12}} \approx 38 \tag{26}$$

The tolerable FER requires less number of WR switch layers compared with the result from the transfer latency requirement. Hence, the maximum number of switch layers for two types messages are 8 and 38, when one lost B2B related frame is tolerable every two months.

B. Firmware Running on LM32

The test setup was used to check whether the B2B firmware running on the LM32 of the SCUs meets the time constraints of the B2B transfer system.

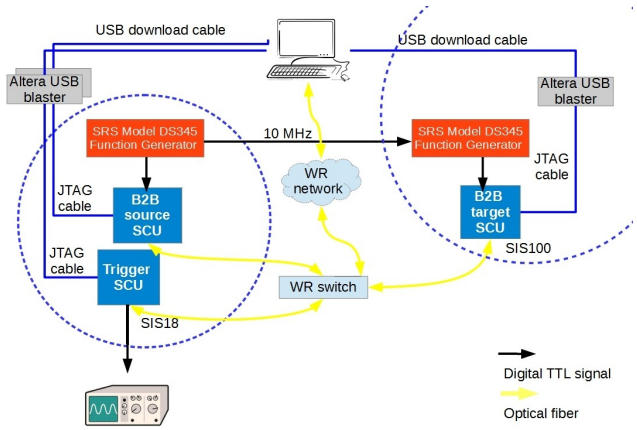

FIG. 13. Schematic of the test setup.

Fig. 13 shows the schematic of the test setup. In this test setup, two SRS MODEL DS345 Synthesized Function Generators (short: DS345) were used to simulate the rf systems of the SIS18 and SIS100. The two DS345s needed to be synchronized to a common reference clock. For simplicity, the DS345 of the SIS100 used a 10 MHz clock from the DS345 of the SIS18 as an external reference clock. The B2B source SCU, the B2B target SCU and the Trigger SCU were connected to a WR switch via single mode fibers, which connected to the WR network. A personal computer (PC) was connected to the WR network, which was a Linux PC installed with the FEC tools, the Altera's Quartus II software and the packETH software. The SCUs were connected to the PC via the Altera USB-Blaster Joint Test Action Group (JTAG) programmer. The PC was used to simulate the DM to produce the B2B start timing message. Besides, the PC monitored the status of the firmware in all SCUs and

measured the running time of the firmware by the SignalTap II Logic Analyzer feature within the Quartus II software. Two DS345s outputted signals to an oscilloscope, together with an output signal from the trigger SCU. Fig. 14 shows the front view of the test setup.

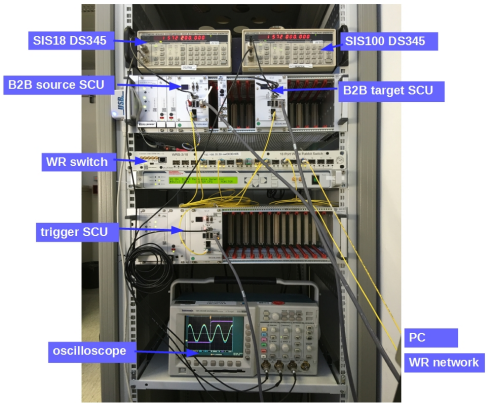

FIG. 14. Front view of the test setup.

From the functional perspective, the B2B source and target SCUs measure the phase of the signals from two DS345, after they receive the B2B start timing message from the PC. Then the phase measurement of the target ring will be transferred from the B2B target SCU to the B2B source SCU. After receiving the message containing the phase measurement, the B2B source SCU calculates the start of the synchronization window and then distributes the start of the synchronization window to the trigger SCU via the WR network. When the trigger SCU receives the message containing the start of the synchronization window, it produces a TTL signal output to the oscilloscope, indicating the phase alignment of two signals from the DS345s. During the process, the running time of some tasks of the firmware was measured by the SignalTap II Logic Analyzer, see Tab. VII.

TABLE VII. Task running time of the firmware on LM32 of the B2B source SCU

Task	Average running time	Worst-case running time
Timing message detection	336 ns	336 ns
Timing message reading	2.7 µs	2.7 µs
Start of the synchronization window calculation	12.6 µs	12.8 µs
Timing message sending	3.2 µs	3.2 µs

According to the task running time measurement result, the time consumption of the timing message detection, reading or sending is shorter than 3 µs, 3% of 100 µs. The calculation time of the start of the synchronization window is much less than 100 µs. Hence, the B2B firmware running on LM32 meets the timing constraints of the B2B transfer.

VI. SIS18 EXTRACTION AND SIS100 INJECTION KICKER TRIGGER SCENARIO

The B2B transfer needs a fast beam extraction and injection, which extracts and injects the beam in a single-turn. Hence, a pulsed kicker magnet must be used with rapid rise time and fall time and the variable pulse flat-top [27]. Fig. 15 shows the schematic diagram of a kicker magnet. The energy storage module is charged with a high voltage power supply. It will be discharged via the transmission cable and the kicker magnet by using the pulse start switch. The length of the flat-top can be modified by switching on the stop switch in correlation with the pulse start switch. Before the increase of the magnetic field, there exist a preparation time for the kicker magnet. The kicker control electronic produces the ignition signal to switch on/off two switches. Generally a preparation time of FAIR kickers is within the 5−10 µs range. Compared with the FAIR rf frequency in the MHz range, a preparation time is not negligible.

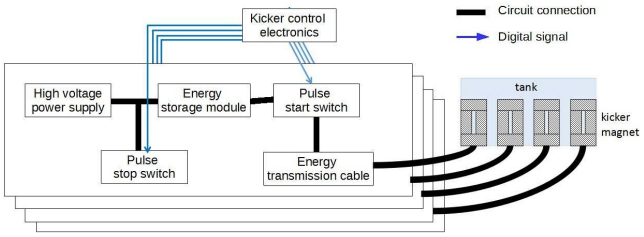

FIG. 15. Schematic diagram of a kicker magnet.

The SIS18 extraction kicker consists of nine kicker magnets. In the existing topology, five kicker magnets are evenly distributed in a tank (the 1^{st} tank) and the other four kicker magnets are evenly distributed in another tank (the 2^{nd} tank). The width of each kicker magnet is 0.25 m and the distance between two kicker magnets is 0.09 m. The distance between the two tanks is 19.17 m [28]. The rise time of the kicker magnet t_{rise} is approximately 90 ns [29]. Bunches are firstly kicked by kicker magnets in the 1^{st} tank and than kicked by the kicker magnets in the 2^{nd} tanks to the transfer line. The SIS100 injection kicker consists of six kicker magnets, which are evenly distributed in a common tank. The width of each kicker magnet is 0.22 m and the distance between two magnets is 0.23 m. The rise time of the kicker magnet t_{rise} is 130 ns [29].

Three ion beams, 4 GeV/u H^+, 200 MeV/u U^{28+} and 970 MeV/u U^{73+}, are used to check the instantaneous trigger of kicker magnets in a common tank, because these ion species have the most stringent requirements. In order to instantaneous trigger of kicker magnets in one tank, the bunch tail passing time from one side to another side of a tank plus the kicker rise time must be shorter than the bunch gap, namely

$$\frac{tank\_length}{\beta c} + rise\_time < bunch\_gap \qquad (27)$$

For the SIS18 and SIS100 kickers, there are the following technical constraints.

- The SIS18 kicker magnets in each tank can be triggered simultaneously when the bunch gap is at least 25% of the cavity rf period.
- The six SIS100 injection kicker magnets can be fired instantaneously for all ion beams, when the bunch gap is at least 35% of the cavity rf period.

In addition, the maximum triggering delay between SIS18 kicker magnets in the two tanks occurs when the kicker magnets in the 1^{st} tank are triggered simultaneously when the tail of a bunch passes by the 1^{st} tank completely and the kicker magnets in the 2^{nd} tank are simultaneously triggered 90 ns before the head of the next bunch to be extracted passes by it. The minimum triggering delay occurs when the kicker magnets in the 1^{st} tank are simultaneously triggered 90 ns before the head of the bunch to be extracted passes by it and the kicker magnets in the 2^{nd} tank are simultaneously triggered when the last bunch passes by the 2^{nd} tank. According to the calculation, the kicker magnets in the 2^{nd} tank can be simultaneously triggered a fixed delay to the simultaneous trigger of the kicker magnets in the 1^{st} tank for all ion beams, when the bunch gap is at least 25% of the cavity rf period, e.g. 80 ns.

VII. APPLICATION

For the FAIR B2B transfer system, both the phase shift and frequency beating methods are applicable. However, many FAIR accelerator pairs can only use the frequency beating method because of the non-integer ratio of the circumference between two rings. Besides, FAIR has many use cases of the B2B transfer that the extraction and injection beam have different energy because of targets installed between two rings. In this case, the beam revolution frequency ratio between the small and large accelerators is used to calculate the synchronization frequencies instead of the circumference ratio between the large and small accelerators. Therefore, the FAIR B2B transfer system with the frequency beating method is applied for all FAIR use cases, see Tab. VIII.

Tab. VIII shows that for most primary beam transfers of FAIR use cases, the B2B transfer with the B2B injection center mismatch less than $\pm 1^\circ$ can be achieved, because the circumference ratio between two rings is an integer or close to an integer. For the B2B transfer between two rings with a far away circumference ratio, the B2B injection center mismatch is $\pm 1.2^\circ$, which is just beyond the specification and still acceptable. However, the system is also required for the FAIR use cases that secondary beams are generated by the pbar target, the FRS or the Super-FRS with an arbitrary energy ratio between the primary and secondary beams. For the rare isotope beam (RIB) transfer from the SIS100 to the CR via the Super-FRS with the 1.5 GeV/u primary beam energy and the 740 MeV/u secondary beam energy, the B2B injection center mismatch is only $\pm 2.1^\circ$ by coincidence. For the antiproton B2B transfer from the SIS100 to the CR via the pbar target and the RIB transfer form the SIS18 to the ESR via the FRS, the B2B injection center mismatch is as large as $\pm 30^\circ$, which is far beyond the upper bound injection center mismatch. For detailed parameters of the FAIR B2B transfer use cases, please see Appendix. B

VIII. CONCLUSION

The concept of the FAIR B2B transfer system and its application for all FAIR use cases were presented, as well as the systematic investigation from the timing, beam dynamics and kicker perspectives. The new FAIR B2B transfer system fulfills the requirements for FAIR.

For the B2B transfer from the SIS18 to the SIS100 with the phase shift method, the sinusoidal rf frequency modulation is a better choice compared with the same periodical parabolic modulation. It needs 7 ms for the SIS18 200 MeV/u U^{28+} and 50 ms for the SIS18 4 GeV/u H^+ to achieve the phase shift of π in order to guarantee a bucket area factor larger than 80% and an adiabaticity smaller than 10^{-4}.

Two test setups were built to verify the timing constraints. The first test setup was used to characterize the WR network for the B2B transfer. If for instance one lost frame is tolerable every two month, the maximum 38 WR switches can be used between the B2B related SCUs and the DM and the maximum 8 WR switches can be used between the B2B related SCUs. In the second test setup, the firmware of the FAIR B2B transfer system was evaluated, running on the soft CPU, LatticeMico32, of the SCUs. The measurement results show that the firmware running on the LatticeMico32 of the SCUs meets the requirement of the timing constraints.

In addition, the boundary conditions of the different trigger scenarios of the SIS18 extraction and SIS100 injection kicker magnets were investigated. The SIS18 kicker magnets in each tank can be triggered simultaneously when the bunch gap is at least 25% of the cavity rf period. The four SIS18 kicker magnets in the 2^{nd} tank can be triggered a fixed delay to the trigger of the five SIS18 kicker magnets in the 1^{st} tank for all ion beams, when the bunch gap is at least 25% of the cavity rf period. The six SIS100 injection kicker magnets can be fired instantaneously, when the bunch gap is at least 35% of the cavity rf period.

For all primary beam transfers of FAIR use cases, the B2B injection center mismatch ($< \pm 1.2^\circ$) is acceptable. However, for the FAIR use cases of the secondary beams,

TABLE VIII. Application of the FAIR B2B transfer system for FAIR accelerators with the frequency beating method

No.	FAIR use cases	B2B injection center mismatch	C^l/C^s	f^s_{rev}/f^l_{rev}	Remark
1	Four batches, each of two SIS18 U^{28+} bunches (200 MeV/u) → eight out of ten SIS100 buckets	±0.4°	5		The FAIR use cases 1-5 have the B2B injection center mismatch smaller than the upper bound ±1°, because the circumference ratio between two rings is an integer or close to an integer.
2	Four batches, each of one SIS18 H^+ bunch (4 GeV/u) → four out of ten SIS100 buckets	±0.4°	5		
3	Two of four SIS18 bunches (30 MeV/u) → two ESR buckets	±0.5°	2-0.003		
4	One SIS18 H^+ bunch (400 MeV/u) → one ESR bucket	±0.5°	2-0.003		
5	One ESR bunch (30 MeV/u) → one CRYRING bucket	±0.5°	2-0.003		
6	One CR antiproton bunch (3 GeV/u) → one HESR bucket	±1.2°	2.6-0.003		The B2B injection center mismatch is just beyond the specification, but it is still acceptable. Although the circumference ratio between two rings is far away from an integer.
7	One CR RIB bunch (740 MeV/u) → one HESR bucket	±1.2°	2.6-0.003		
8	One SIS100 H^+ bunch (28.8 GeV/u) $\xrightarrow[\text{target}]{\text{par}}$ (3 GeV/u) one CR bucket	±41.5°	not applicable	arbitrary	The B2B injection center mismatch is far beyond the specification, because the energy ratio before and after targets is arbitrary. (The FAIR use case No. 8 is close to the specification and still acceptable by coincidence.)
9	One SIS100 RIB bunch (1.5 GeV/u) $\xrightarrow{\text{Super-FRS}}$ (740 MeV/u) one CR bucket	±2.1°	not applicable	arbitrary	
10	One SIS18 RIB bunch (550 MeV/u) $\xrightarrow{\text{FRS}}$ (400 MeV/u) one ESR bucket	±31.2°	not applicable	arbitrary	

the mismatch is as large as ±30°.

The important investigations for the FAIR B2B transfer system were discussed in this manuscript. However, there are still some investigations which are required for the final system operation. The magnetic horn after the pbar target has to be synchronized with the antiproton beam to the "us" order of magnitude. The bunch compressor of the SIS100 has to be synchronized the beam extraction. Finally, for the FAIR use cases of the secondary beam with the B2B injection center mismatch larger than ±30°, the FAIR B2B transfer system with specific beam accumulation methods (e.g. the barrier bucket or the unstable fixed point accumulation) has to be checked.

The realistic test of the system on FAIR accelerators will be done at the end of 2018, because many FAIR technical basis and rings are still under construction.

IX. ACKNOWLEDGMENTS

The author would like to thank T. Ferrand for his contribution of the development of the LLRF system for the B2B transfer system for FAIR. The author would also like to acknowledge Prof. Dr. O. Kester for his support, as well as Dr. D. Ondreka and Dr. D. Beck for their supervision. Besides, the author expresses the sincere gratitude to colleagues from the CSCO and PBRF departments, GSI, for their technical support. I am especially grateful for the CSCO timing group member C. Prados, who defined the test scenario of the WR network of the FAIR GMT system. The gratitude also extends to colleagues from the SBES, PBHV, SHE-P departments, GSI.

[1] CERN accelerator complex, . URL https://home.cern/about/accelerators.

[2] H. Damerau. Lecture Note: Timing, Synchronization & Longitudinal Aspects. *CERN Accelerator School*, 2017. URL https://cas.web.cern.ch/cas/IET2017/Lectures/DamerauI.pdf.

[3] J-PARC, 2016. URL https://www.kek.jp/en/Facility/ACCL/J-PARC/.

[4] F. Tamura, A. Schnase, M. Nomura, M. Yamamoto, and K. Hasegawa. Synchronization System for the J-PARC RCS. In *Proc. of 3rd Annual Meeting of Particle Accelerator Society of Japan*, Tokyo, Japan, 2006. URL http://www.pasj.jp/web_publish/pasj3_lam31/Proceedings/W/WP64.pdf.

[5] J. Eschke. International Facility for Antiproton and Ion Research (FAIR) at GSI, Darmstadt. *Journal of Physics G: Nuclear and Particle Physics*, 31(6):S967, 2005. URL http://iopscience.iop.org/article/10.1088/0954-3899/31/6/041/meta.

[6] FAIR - Facility for Antiproton and Ion Research, 2011. URL https://www.gsi.de//forschungbeschleuniger/fair.htm.

[7] F. Nolden and et al. The Collector Ring CR of the FAIR Project. In *Proc. of EPAC*, Edinburgh, Scotland, 2006. URL http://accelconf.web.cern.ch/AccelConf/e06/PAPERS/MOPCH077.PDF.

[8] R. Bär and et al. Technical Design Report on the Collector Ring. *GSI Internal Document*, 2013. URL https://indico.gsi.de/getFile.py/access?resId=7&materialId=slides&confId=2200.

[9] P. Spiller and G. Franchetti. The FAIR Accelerator Project at GSI. *Nuclear Instruments and Methods in Physics Research Section A: Accelerators, Spectrometers, Detectors and Associated Equipment*, 561(2):305–309, 2006. URL http://www.sciencedirect.com/science/article/pii/S0168900206000507.

[10] M. Steck and et al. Advanced Design of the FAIR Storage Ring Complex. In *Proc. of PAC*, Vancouver, BC, Canada, 2009. URL https://accelconf.web.cern.ch/AccelConf/PAC2009/papers/fr1gri03.pdf.

[11] U. Krause, V. Schaa, and R. Steiner. The GSI Control System. In *Proc. of ICALEPCS*, volume 91, 1991. URL http://www.iaea.org/inis/collection/NCLCollectionStore/_Public/25/028/25028669.pdf.

[12] R. Huhmann and et al. The FAIR Control System-System Architecture and First Implementations. In *Proc. of ICALEPCS*, San Francisco, California, USA, 2013. URL http://epaper.kek.jp/ICALEPCS2013/papers/moppc097.pdf.

[13] D. Beck and et al. The new White Rabbit based Timing System for the FAIR Facility. In *Proc. of PCaPAC*, Kolkata, India, 2012. URL http://accelconf.web.cern.ch/Accelconf/pcapac2012/papers/fria01.pdf.

[14] K. Kaiser. F-TN-C-008e, Detailed Documentation of the Scalable Control Unit SCU3 FG 900.112. *FAIR Technical Note*, 2014.

[15] P. Moritz. BuTiSDevelopment of a Bunchphase Timing System. *GSI Scientific Report*, 2006. URL http://citeseerx.ist.psu.edu/viewdoc/download?doi=10.1.1.162.1765&rep=rep1&type=pdf.

[16] P. Moritz. F-CS-RF-14e BuTiS, Common Specification on the Bunch Phase Timing System (BuTiS). *FAIR Common Specification*, 2012.

[17] H. Klingbeil. Detailed Specification on the LLRF DSP System for FAIR Ring RF Systems. *GSI Internal Document*, 2013.

[18] J. Bai and T. Ferrand. F-TC-C-05, Concept of the FAIR Bunch To Bucket Transfer System. *FAIR Technical Concept*, 2016.

[19] C. Bovet, R. Gouiran, K.H. Reich, and I. Gumowski. A Selection Of Formula And Data Useful For The Design Of AG Synchrotrons. Technical report, CERN, 1970. URL http://cds.cern.ch/record/280305/files/cm-p00041563.pdf.

[20] S. Y. Lee. *Accelerator Physics*. WORLD SCIENTIFIC, Singapore, 3 edition, 2011. ISBN 978-981-4374-94-1 978-981-4374-95-8. URL http://www.worldscientific.com/worldscibooks/10.1142/8335.

[21] E. Ezura, M. Yoshii, F. Tamura, and A. Schnase. Beam-Dynamics View of RF Phase Adjustment for Synchronizing J-PARC RCS with MR or MLF. *KEK Internal Document*, 2008. URL http://ccdb5fs.kek.jp/tiff/2008/0826/0826001.pdf.

[22] H. Liebermann and D. Ondreka. FAIR and GSI Reference Cycles for SIS18. *GSI Internal Document*, 2013.

[23] T. Ferrand. *Development of the LLRF System for a Deterministic Bunch-to-Bucket Transfer for FAIR*. (Unpublished doctoral thesis), Technical University Darmstadt, Germany.

[24] Datasheet of Draka Optical fiber, . URL http://www.drakauc.com/ucfibre-optical-patchcords/.

[25] D. Beck. Timing Messages of GMT System for FAIR, 2015. URL https://www-acc.gsi.de/wiki/Timing/TimingSystemEvent.

[26] C. Prados and J. Bai. Testing the WR Network of the FAIR General Machine Timing System. *GSI Internal Document*, 2016.

[27] I. Petzenhauser and et al. Concept and Design of the Injection Kicker System for the FAIR SIS100 Synchrotron. In *Proc. of IPAC*, Busan, Korea, 2016.

[28] J. Roß. SIS18 Sektoren Technische Zeichnungen und Fotografien. *GSI Internal Document*, 2008.

[29] U. Blell. F-DS-IE-03e, Detailed Specification of the SIS100 Injection Kicker Magnets and their Pulse Power Supplies. *FAIR Detailed Specification*, 2014.

Appendix A: Traffic produced by the XenaBay ports of the test setup

TABLE IX. Traffic produced by the XenaBay ports of the test setup
Adapted from "Testing the WR Network of the FAIR General Machine Timing System" by C. Prados and J. Bai, 2016, GSI Internal Document.

Switch	XenaBay Port	Traffic	Ethernet frame size (bytes)	VLAN	Priority	Usage
WR switch 1	Port 1	100 Mbit/s	110	7	7	Control massage Broadcast
	Port 2					
	Port 3	10 Mbit/s	110	7	7	Control massage Unicast
	Port 4					
	Port 5					
	Port 6	1 Mbit/s	64 - 1518	5	5	Management Broadcast
WR switch 2	Port 7	2 Mbit/s	64 - 1518	5	5	Management Broadcast
	Port 8					
	Port 9					
	Port 10	1 Mbit/s	64 - 1518	5	5	Management Broadcast
WR switch 3	Port 11					
	Port 12					
	Port 13	2 Mbit/s	64 - 1518	5	5	Management Broadcast
	Port 14	1 Mbit/s	64 - 1518	5	5	Management Broadcast
WR switch 4	Port 15	1 Mbit/s	64 - 1518	5	5	Management Broadcast
	Port 16	25 kbit/s	110	6	6	B2B Broadcast
	Port 17	5 kbit/s	110	7	7	B2B Unicast
	Port 18	2 Mbit/s	64 - 1518	5	5	Management Broadcast
Broadcast: messages are sent by one port and sent to all other ports. Unicast: messages are sent by one port and sent to a specific port.						

Appendix B: Parameters of FAIR B2B transfer use cases

1. Parameters of the B2B Transfer from SIS18 to SIS100

TABLE X: Parameters related to the B2B transfer from the SIS18 to the SIS100

		Proton		Heavy Ion U^{28+}	
	Unit	SIS18 Ext	SIS100 Inj	SIS18 Ext	SIS100 Inj
Design orbit	m	216.72	1083.6	216.72	1083.6
$C_{SIS18} : C_{SIS100}$		5		5	
Ext kinetic energy	MeV/u	4000		200	
Inj kinetic energy	MeV/u		4000		200
h		1	10(1×4)	2	10(2×4)
f_{rf}	MHz	1.359358	2.718715	1.572536	1.572536
T_{rf}	µs	0.736	0.368	0.636	0.636
f_{rev}	MHz	1.359358	0.271872	0.786268	0.157254
T_{rev}	µs	0.736	3.678	1.272	6.359
Max $\Delta p/p$		±0.008	±0.01	±0.008	±0.01
$\Delta R/R$		$\pm 0.8 \times 10^{-4}$		$\pm 2.4 \times 10^{-4}$	
$\eta = \frac{1}{\gamma^2} - \alpha_p$		0.026		0.647	
γ_t		10		5.8	
α_p		0.010		0.030	
β		0.982	0.982	0.568	0.568
γ		5.294	5.294	1.215	1.215
Q_x		4.17		4.17	
Q_y		3.4		3.4	
$Q_x^{'}$		-7.5		-6.5	

$Q_y^{'}$		-4.4		-4.1	
		Injection four times		Injection four times	

2. Parameters of the B2B Transfer from SIS18 to ESR

TABLE XI: Parameters related to the B2B transfer from the SIS18 to the ESR

		Proton/Heavy Ion		Heavy Ion	
	Unit	SIS18 Ext	ESR Inj	SIS18 Ext	ESR Inj
Design orbit	m	216.72	108.36	216.72	108.36
Inj orbit	m		108.36+0.15		108.36+0.15
$C_{SIS18} : C_{ESR}$		1.997		1.997	
Ext kinetic energy	MeV/u	550		30	
Inj kinetic energy	MeV/u		400		30
h		1	1	4	2
f_{rf}	MHz	0.989756	1.976777	1.373201	1.371302
T_{rf}	µs	1.010	0.506	0.728	0.879
f_{rev}	MHz	0.989756	1.976777	0.343300	0.685651
T_{rev}	µs	1.010	0.506	2.913	1.458
$\Delta p/p$ compared with design orbit			1%		1%
$\Delta R/R$			0.138%		0.138%
$\eta = \frac{1}{\gamma^2} - \alpha_p$		0.480	0.310	0.909	0.759
γ_t		10	2.357	5.8	2.357
α_p		0.010	0.18	0.030	0.18
β		0.715	0.715	0.248	0.248
γ		1.429	1.429	1.032	1.032
		Accumulation beam in injection orbit		Accumulation beam in injection orbit	

3. Parameters of the B2B Transfer from SIS18 to ESR via the FRS

TABLE XII: Parameters related to the B2B transfer from the SIS18 to the ESR via the FRS

		Heavy Ion Beam	Rare Isotope Beam
	Unit	SIS18 Ext	ESR Inj
Design orbit	m	216.72	108.36
Inj orbit	m		108.36+0.15
$C_{SIS18} : C_{ESR}$		1.997	
Ext kinetic energy	MeV/u	550	
Inj kinetic energy	MeV/u		400
h		1	1
f_{rf}	MHz	1.076965	1.976777
T_{rf}	µs	0.929	0.506
f_{rev}	MHz	1.076965	1.976777
T_{rev}	µs	0.929	0.506
$\Delta p/p$ compared with design orbit			1%
$\Delta R/R$			0.138%
$\eta = \frac{1}{\gamma^2} - \alpha_p$		0.366	0.310
γ_t		5.8	2.357
α_p		0.030	0.18
β		0.778	0.715
γ		1.590	1.429
		One time injection	

4. Parameters of the B2B Transfer from ESR to CRYRING

TABLE XIII: Parameters related to the B2B transfer from the ESR to the CRYRING

		Proton/Antiproton	Heavy Ion

	Unit	ESR Ext	CRYRING Inj	ESR Ext	CRYRING Inj
Design orbit	m	108.36	54.18	108.36	54.18
Ext orbit	m	108.36+0.15		108.36+0.15	
$C_{ESR} : C_{CRYRING}$		2.003		2.003	
Ext kinetic energy	MeV/u	30		4-10	
Inj kinetic energy	MeV/u		30		4-10
h		1	1	1	1
f_{rf}	MHz	0.685651	1.373200	0.254354-0.400885	0.509507-0.802879
T_{rf}	µs	1.458	0.728	3.932-2.494	1.963-1.246
f_{rev}	MHz	0.685651	1.373200	0.254354-0.400885	0.509507-0.802879
T_{rev}	µs	1.458	0.728	3.932-2.494	1.963-1.246
$\eta = \frac{1}{\gamma^2} - \alpha_p$		0.759		0.798-0.812	
γ_t		2.357		2.357	
α_p		0.18		0.18	
β		0.248	0.248	0.092-0.145	0.092-0.145
γ		1.032	1.032	1.004-1.011	1.004-1.011
		One time injection		One time injection	

5. Parameters of the B2B Transfer from CR to HESR

TABLE XIV: Parameters related to the B2B transfer from the CR to the HESR

		Proton→ Antiprotron		Heavy Ion→ RIB	
	Unit	CR Ext	HESR Inj	CR Ext	HESR Inj
Design orbit	m	221.45	575	221.45	575
$C_{HESR} : C_{CR}$		2.597		2.597	
Ext kinetic energy	GeV/u	3		0.74	
Inj kinetic energy	GeV/u		3		0.74
h		1	1	1	1
f_{rf}	MHz	1.316775	0.507131	1.124408	0.433043
T_{rf}	µs	0.759	1.972	0.889	2.309
f_{rev}	MHz	1.316775	0.507131	1.124408	0.433043
T_{rev}	µs	0.759	1.972	0.889	2.309
Max $\Delta p/p$		±3%		±1.5%	
$\eta = \frac{1}{\gamma^2} - \alpha_p$		-0.011		0.178	
γ_t		3.85		2.711	
α_p		0.067			
β		0.972	0.972	0.830	0.830
γ		4.221	4.221	1.794	1.794
		100 times Injection per 10 seconds		100 times Injection per 10 seconds	

6. Parameters of the B2B Transfer from SIS100 to CR

TABLE XV: Parameters related to the B2B transfer from the SIS100 to the CR

		Proton→ Antiprotron		Heavy Ion→ RIB	
	Unit	SIS100 Ext	CR Inj	SIS100 Ext	CR Inj
Design orbit	m	1083.6	221.45	1083.6	221.45
$C_{SIS100} : C_{CR}$		4.893		4.893	
Ext kinetic energy	GeV/u	28.8		1.5	
Inj kinetic energy	GeV/u		3		0.74
h		5(1 bunch)	1	2(1 bunch)	1
f_{rf}	MHz	1.383509	1.316778	0.511628	1.124408
T_{rf}	µs	0.723	0.759	1.955	0.889
f_{rev}	MHz	0.276702	1.316778	0.255814	1.124408
T_{rev}	µs	3.614	0.759	3.909	0.889
Max $\Delta p/p$		±3%		±1.5%	
β		0.9995	0.972	0.924	0.830
γ		31.918	4.221	2.610	1.794

		One time injection	One time injection